Global NEST Journal, Vol 10, No 1, pp 1-7, 2008

ENHANCEMENT OF PHOTOCATALYTIC ACTIVITY OF TiO_2 NANOPARTICLES BY SILVER DOPING: PHOTODEPOSITION VERSUS LIQUID IMPREGNATION METHODS

M.A. BEHNAJADY*
N. MODIRSHAHLA
M. SHOKRI
B. RAD

Department of Applied Chemistry
Islamic Azad University
Tabriz Branch
P.O. Box 1655, Tabriz, I.R. Iran

Received: 04/10/07
Accepted: 29/11/07

*to whom all correspondence should be addressed:
Fax: +984113313922; e-mail: behnajady@iaut.ac.ir

ABSTRACT

Silver doped TiO_2 nanoparticles have been prepared by liquid impregnation (LI) and photodeposition (PD) methods and characterized by surface analytical methods such as scanning electron micrographs (SEM) and X-ray diffraction (XRD). The photocatalytic activity of silver doped TiO_2 was tested by photocatalytic degradation of C.I. Acid Red 88 (AR88) as a model compound from monoazo textile dyes. Results show silver doped TiO_2 is more efficient than undoped TiO_2 at photocatalytic degradation of AR88. The positive effect of silver on the photoactivity of TiO_2 at degradation of AR88 may be explained by its ability to trap electrons. This process reduces the recombination of light generated electron-hole pairs at TiO_2 surface. Silver content has an optimum value 2% in LI and 0.5% in PD methods for achieving high photocatalytic activity. The AR88 decomposition with Ag-photodeposited method was much higher than that of deposited with LI method.

KEYWORDS: Heterogeneous photocatalysis, TiO_2 nanoparticles, Silver doping, Photodeposition method, Liquid impregnation method, C.I. Acid Red 88.

1. INTRODUCTION

Heterogeneous photocatalysis is a promising method among advanced oxidation processes (AOPs), which can be used for degradation of various organic pollutants in water and wastewater (Behnajady *et al*., 2006; Daneshvar *et al.*, 2004; Behnajady *et al.,* 2007a; Behnajady *et al.*, 2007b). In photocatalysis systems a combination of semiconductors (such as TiO_2, ZnO, F_2O_3, CdS and ZnS) and UV or visible lights can be used. Upon irradiation, valence band electrons are promoted to the conduction band leaving a hole behind. These electron-hole pairs can either recombine or interact separately with other molecules. The holes at the valence bond, having an oxidation potential of +2.6 V versus normal hydrogen electrode (NHE) at pH=7, can oxidize water or hydroxide to produce hydroxyl radicals (Behnajady *et al.,* 2006).

The limitation of the rate of photocatalytic degradation is attributed to the recombination of photogenerated electron-hole (e^--h^+) pairs. Various attempts have been made to reduce e^--h^+ recombination in photocatalytic processes. These studies include doping metal ions into the TiO_2 lattice (Sakhtivel *et al.*, 2004; Subba Rao *et al.*, 2003) and coupling semiconductors (Wu, 2004). Sakhtivel *et al.* (2004) have showed that the photonic efficiency of Pt deposited on TiO_2 is almost comparable with Au/TiO_2 but higher than Pd/TiO_2. In this work, the highest photonic efficiency was observed with metal deposition level of less then 1 wt%. Kondo and Jardim (1991) have showed the Ag-loaded TiO_2 was more effective than the pure TiO_2 in the degradation of chloroform and urea. Also, Sahoo *et al.* (2005), found that Ag^+ doped TiO_2 is slightly more efficient than the undoped TiO_2 in the photocatalytic degradation of C.I. Basic Violet 3.

The objective of the present study is to prepare silver doped TiO_2 nanoparticles by LI and PD methods with different values of silver deposited on TiO_2 surface for determining of optimum metal loading and also to compare the activity of the silver doped TiO_2 prepared with different methods at degradation of C.I. Acid Red 88 (AR88) as a model compound.

2. EXPERIMENTAL

2.1. Materials

AR88 as a model pollutant from textile industry was purchased from ACROS organics (USA). The AR88 is a monoazo anionic dye with C.I. number 15620 and λ_{max} 506 nm. The TiO_2 sample was purchased from Degussa, Germany (TiO_2-P25). $AgNO_3$ and $HClO_4$ were purchased from Fluka.

2.2. The preparation of silver doped TiO_2 nanoparticles

2.2.1. Liquid impregnation method

In the LI method silver ion (Ag^+) doped on TiO_2 was prepared according to the following steps. First, 3 g of TiO_2 was added to 100 ml deionized water. Then the required amount of $AgNO_3$ for doping was added to TiO_2 suspension, where the silver concentration was of 0.5, 1.0, 1.5, 2.0 and 2.5% (mole ratio) versus TiO_2. The slurry was stirred well and allowed to rest for 24 h and then dried in an air oven at 100 ^oC for 12 h. The dried solids were ground in an agate mortar and calcined at 400 ^oC for 6 h in a furnace (Sahoo *et al.*, 2005).

2.2.2. Photodeposition method

In the PD method Ag metal doped on TiO_2 was prepared by photoreducing Ag^+ ions to Ag metal on the TiO_2 surface according to the following steps. First, 3.0 g of TiO_2 was added to 100 ml deionized water. The pH of the TiO_2 suspension was adjusted to 3 by addition of perchloric acid. Then the required amount of $AgNO_3$ for doping was added to the TiO_2 suspension, where the silver concentration was of 0.5, 1.0, 1.5, 2.0 and 2.5% (mole ratio) versus TiO_2. The mixtures were then irradiated with UV light (30 W, UV-C, λ_{max} = 254 nm, manufactured by Philips, Holland) for 3 h and then dried in an air oven at 100 ^oC for 12 h. The dried solids were ground in an agate mortar and calcined at 400 ^oC for 6 h in a furnace (Sobana *et al.*, 2006).

2.3. The characterization of TiO_2 nanoparticles

The crystalline phase and particle size of TiO_2 nanoparticles (doped and undoped) were analyzed by X-ray diffraction (XRD) measurements which were carried out at room temperature by using Siemens X-ray diffraction D5000 with Cu Kα radiation (λ = 0.15478 nm). The SEM image of doped and undoped TiO_2 were recorded with SEM LEO 440 i.

2.4. Photoreactor

Photocatalytic degradation was performed in a batch quartz photoreactor of 100 ml volume with UV lamp (15 W, UV-C, λ_{max} = 254 nm, manufactured by Philips, Holland) in vertical array, which was placed in front of the quartz tube reactor. So when the light intensity was measured by Lux-UV-IR meter (Leybold Co.) maximum intensity was observed.

2.5. Procedure

In the photocatalytic degradation of AR88 a solution which contains AR88 and different types of TiO_2 nanoparticles (doped and undoped) were prepared and agitated for 30 min in the darkness, then 100 ml of the above suspension was transferred into the photoreactor and then O_2 was bubbled through the reactor with 0.4 ml min^{-1} flow rate. The reaction was initiated when the lamp was switched on and during irradiation, O_2 flow was maintained in the photoreactor to keep the suspension homogeneous, then at certain reaction intervals, 5 ml of sample was withdrawn, centrifuged and the concentration of AR88 was determined by means of a UV-vis spectrophotometer (Ultrospec 2000, England) at 506 nm.

3. RESULTS AND DISCUSSION

3.1. The characterization of TiO_2 and silver doped TiO_2 nanoparticles

The SEM pictures of pure TiO_2, 2% Ag^+-TiO_2 (prepared with LI method) and 0.5% Ag-TiO_2 (prepared with PD method) are shown in Figure 1. The SEM pictures shows that the distribution of silver on the surface of TiO_2 is not uniform and silver doped TiO_2 catalyst contains irregular shaped particles which are the aggregation of tiny crystals.

The XRD patterns of different TiO_2 nanoparticles (pure and silver doped) were shown in figure 2, for 2θ diffraction angles between 5^o and 70^o. The XRD pattern of TiO_2 shows five primary peaks at 25.2^o, 38^o, 48.2^o, 55^o and 62.5^o which can be attributed to different diffraction planes of anatase TiO_2. Four different peaks at 27.5^o, 36^o, 54^o, and 69^o can be attributed to different diffraction planes of rutile form of TiO_2.

Table 1. Crystal size of TiO_2 and silver doped TiO_2

Catalyst	Crystal phase	
	Anatase	Rutile
TiO_2	15.2 nm	14.1 nm
Ag-TiO_2 0.5%	14.4 nm	13.8 nm
Ag^+-TiO_2 2%	13.8 nm	13.7 nm

These results showed that the TiO_2-P25 is almost 80% anatase and 20% rutile. The average particle size (D in nm) of TiO_2 nanoparticles was determined from XRD patterns of different TiO_2 samples (figure 2) according to the Scherrer's equation and were presented in Table 1.

$$D = \frac{k\lambda}{\beta \cos\theta} \quad (1)$$

In this equation, k is a constant equal to 0.89, λ, the X-ray wavelength equal to 0.154 nm, β, the full width at half maximum and θ, the half diffraction angle (Wu, 2004). Results show that the addition of silver did not significantly effect the crystal size. The XRD patterns of silver doped TiO_2 samples almost coincide with that of pure TiO_2 showing no diffraction peaks due to silver doping thus suggesting that the silver dopants are merely placed on the surface of the crystals.

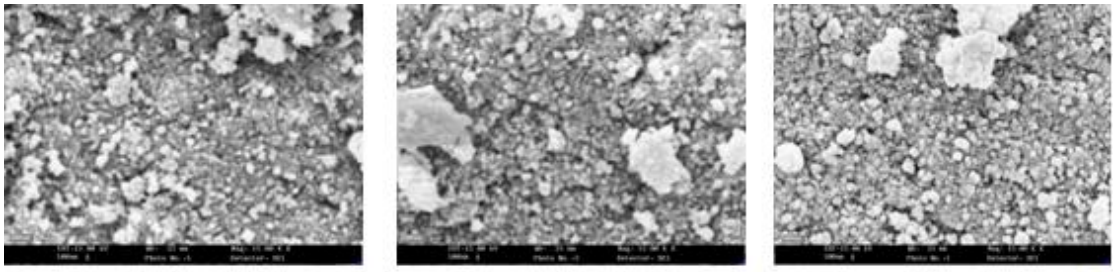

Figure 1. SEM micrographs of (a) undoped TiO_2, (b) 0.5% Ag-TiO2 and (c) 2% Ag^+-TiO2 nanoparticles

3.2. The effect of silver doping on the photocatalytic activity of TiO_2 nanoparticles

The photodecolorization of AR88 in the presence of nanosized-TiO_2 powder (undoped and silver doped) and UV light radiation is thought to be a pseudo first-order kinetic reaction. The semi-logarithmic graphs of the concentration of AR88 in the presence of 300 mg l^{-1} of doped and undoped TiO_2 vs. irradiation time (Figure 3) yield straight lines indicating pseudo first-order reaction. The apparent first-order reaction rate constants (k_{ap}) were evaluated from experimental data using a linear regression.

Figure 3 shows silver doped TiO_2 with PD and LI methods are more efficient than undoped TiO_2 at decolorization AR88. TiO_2 under irradiation of light with wavelength lower than 390 nm produces e^--h^+ pairs. Recombination of e^--h^+ pairs reduces the rate of photocatalytic degradation. The positive effect of silver on the photoactivity of TiO_2 at degradation of AR88 may be explained by its ability to trap electrons. This process reduces the recombination of light generated e^--h^+ at TiO_2 surface (Coleman *et al.*, 2005). Therefore a more effective electron transfer occurs to the electron acceptors and donors adsorbed on the surface of the

particle than in the case of undoped TiO_2. Oxygen adsorbed on photocatalyst surface traps the electrons and produces superoxide anion (Daneshvar *et al.*, 2004). On the other hand holes at the TiO_2 surface can oxidize adsorbed water or hydroxide ions to produces hydroxyl radicals (Behnajady *et al.*, 2007a).

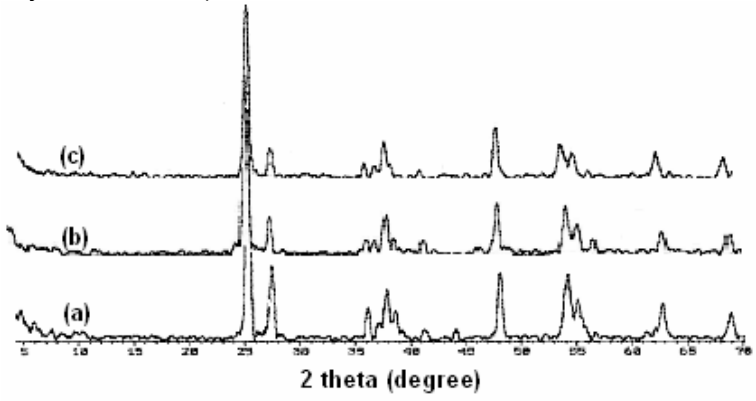

Figure 2. X-ray diffraction patterns of (a) undoped TiO_2,
(b) 0.5% Ag-TiO_2 (with PD method), (c) 2% Ag^+-TiO_2 (with LI method)

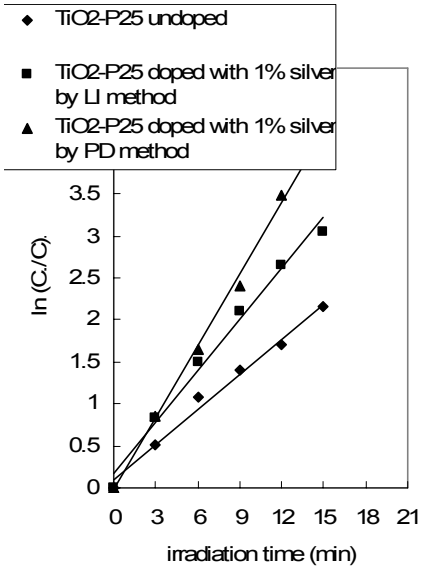

Figure 3. Semi-logarithmic graph of AR88 concentration vs. irradiation time
in the presence of undoped and silver doped TiO_2-P25 nanoparticles
I_o = 37 W m^{-2}, $[AR88]_o$ = 20 mg l^{-1}, $[TiO_2]$ = 300 mg l^{-1}

Results in Figure 3 also show the AR88 decolorization activity of Ag-photodeopsited TiO_2 was much higher than of silver loaded TiO_2 prepared by LI method. The difference in the photoactivity of silver doped TiO_2 prepared with different methods can be discussed in terms of the oxidation state of silver on TiO_2 surface. During the preparation process by PD method, Ag^+ ions in the suspension were reduced to Ag, but in the LI method silver deposited at TiO_2 surface as Ag^+ ions. In the silver doped TiO_2 with LI method (Ag^+-TiO_2), the reduction of silver ions to metallic silver consumes electrons. Therefore the e^--h^+ recombination reduces (Vamathevan *et al.*, 2002). Szabo-Bardos *et al.* (2003) showed that the electron scavenging by the oxygen at the surface of the excited semiconductor particle cannot efficiently compete with the electron transfer to the silver ion. So, the electron transfer to silver ion is a rather fast comparing to electron transfer to oxygen molecule, and therefore the formation of $O_2^{-\bullet}$ is reduced.

But in the silver doped TiO_2 with PD method (Ag-TiO_2), the loading of Ag metals on the TiO_2 surface can expedite the transport of photogenerated electrons to the outer systems

(Sakthivel *et al*., 2004). The transfer of electrons to metal deposits, results in the deposits becoming negatively charged (Vamathevan *et al.*, 2002). In air-equilibrated systems, Ag deposits on the TiO_2 surface enhance photoactivity by accelerating the transfer of electrons to dissolved oxygen molecules.

Therefore reversely Ag^+-TiO_2 system in the Ag-TiO_2, the superoxide anion radical is formed as a result of oxygen reduction by transfer of trapped electrons from Ag metal to oxygen, as can be seen in scheme1.

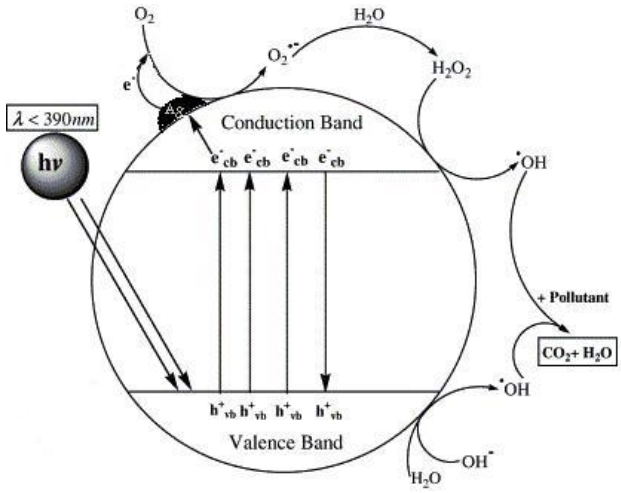

Scheme 1. Mechanism of photocatalysis in Ag deposited TiO_2 with PD method under UV light irradiation

3.3. The effect of doping content of silver

Results in Figure 4 show that silver loading on TiO_2 surface at decolorization of AR88 has an optimum value of 0.5% and 2% for Ag-TiO_2 and Ag^+-TiO_2, respectively. Results show k_{ap} increases with an increase in the silver loading up to optimum loading and then decreases. The detrimental effect of silver on TiO_2 photoactivity has several reasons.

- Excessive coverage of TiO_2 catalyst limits the amount of light reaching to the TiO_2 surface, reducing the number of photogenerated e^--h^+ pairs and lowering consequently the TiO_2 photoactivity (Carp *et al.*, 2004).
- Metal deposits may occupy the active sites on the TiO_2 surface for the desired photocatalytic reactions causing the TiO_2 lose its activity (Coleman *et al.*, 2005).
- Negatively charged silver sites begin to attract holes and subsequently recombine them with electrons. In this case, the metal deposits become recombination centers (Carp *et al.*, 2004).
- The probability of the hole capture is increased by the large number of silver particles at high silver loadings, which decrease the probability of holes reacting with adsorbed species at the TiO_2 surface (Sobana *et al.*, 2006).

3.4. The effect of slurry dosage of TiO_2 and silver doped TiO_2

Results in figure 5 shows the rate constant increases with increasing the amount of TiO_2 until 200 mg l^{-1} for silver doped TiO_2 with PD method and 300 mg l^{-1} for silver doped TiO_2 with LI method and undoped TiO_2 samples. The observed enhancement in this range is probably due to an increased number of available adsorption and catalytic sites on TiO_2 (Behnajady *et al*., 2007a). When the dosage of TiO_2 was increased above the limiting value, the decolorization rate decreased due to an increase in the turbidity of the suspension and a decrease in UV light penetration (Daneshvar *et al.*, 2004; Behnajaby *et al.*, 2007a; 2007b). The same optimum dosage of TiO_2 for silver doped TiO_2 with LI method and undoped TiO_2 samples shows the surface properties of silver doped TiO_2 with LI method is not very different from undoped TiO_2 samples.

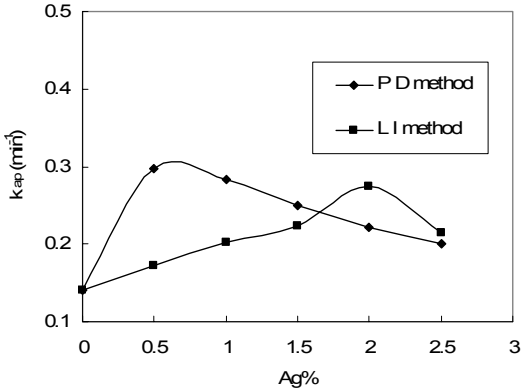

Figure 4. Effect of silver content on the photoactivity of TiO_2-P25 nanoparticles at degradation of AR88
I_o = 37 W m^{-2}, [AR88]$_o$ = 20 mg l^{-1}, [TiO_2] = 300 mg l^{-1}

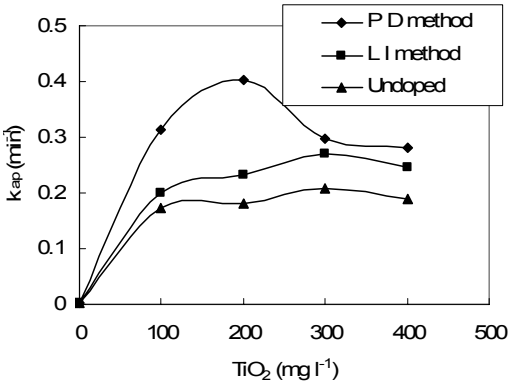

Figure 5. Effect of slurry dosage of undoped and silver doped TiO_2-P25 nanoparticles at degradation of AR88
I_o = 37 W m^{-2}, [AR88]$_o$ = 20 mg l^{-1}

3.5. The effect of re-calcination temperature on the photocatalytic activity of silver doped TiO_2

In order to study the influence of the calcination temperature on the photocatalytic activity of silver doped TiO_2, the 2% silver doped TiO_2 with LI method was re-calcined at 500, 700 and 900 ^oC for 2 h and results are shown in figure 6a. Results in this figure shows the rate constant decreases with increasing the re-calcination temperature. This behavior can be related to the transform of anatase to the rutile phase, which has little photocatalytic activity. As shown in figure 6b, at 700 ^oC exists only the rutile phase and anatase phase disappeared.

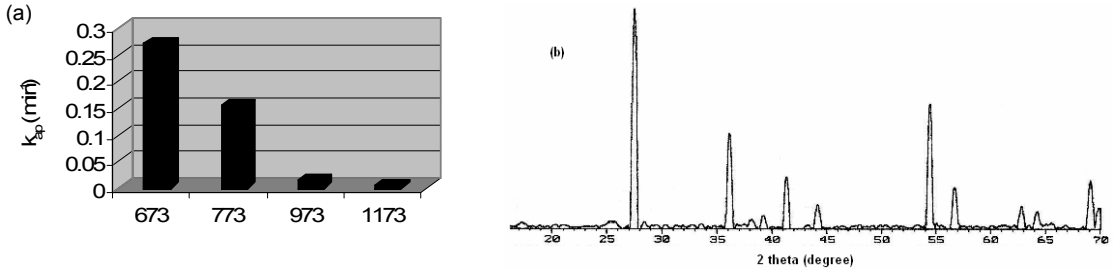

*Figure 6***.** Effect of re-calcination temperature on the photocatalytic activity of silver doped TiO_2-P25 nanoparticles (a), X-ray diffraction patterns of 2% silver doped TiO_2 nanoparticles with LI method re-calcined at 700 ^oC (b)
I_o = 37 W m^{-2}, [AR88]$_o$ = 20 mg l^{-1}, [TiO_2] = 300 mg l^{-1}

3.6. The effect of silver doping on sedimentation profile of TiO_2

The separation of TiO_2 nanoparticles after the treatment process is very difficult. In order to make the environmental application of TiO_2 photocatalysis more practical, immobilization of TiO_2 on a certain substrate is required (Behnajady *et al.,* 2007a). But in the solar systems TiO_2 can be allowed to settle down during the night. Figure 7 shows the effect of silver doping on the sedimentation of TiO_2. The silver doped TiO_2 was satisfactorily sedimented, whereas the undoped TiO_2 did not precipitate. Therefore silver doped TiO_2 nanoparticles could be readily separated from the suspension by only settling and was not necessary to add any coagulant to the system.

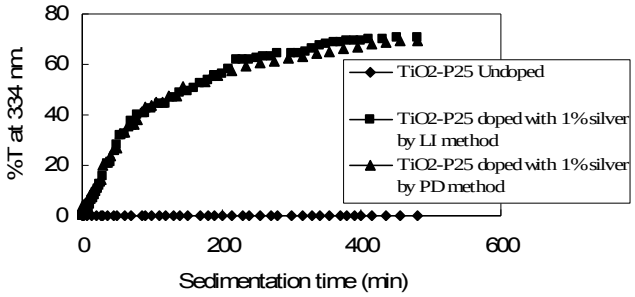

Figure 7. The effect of silver doping on the sedimentation profiles of undoped and silver doped TiO_2-P25 nanoparticles

4. CONCLUSIONS

It was found that silver doped TiO_2 is more efficient than undoped TiO_2 at photocatalytic degradation of AR88. Silver content has an optimum value 2% in LI and 0.5% in PD method for achieving high photocatalytic activity. The AR88 decomposition with Ag-photodeposited method was much higher than that of deposited with LI method. Increasing the calcination temperature reduces the photocatalytic activity and results also show that the silver doped TiO_2 can be separate from treated effluent very easily than undoped TiO_2.

ACKNOWLEDGEMENTS

The authors thank the Islamic Azad University of Tabriz branch for financial and other supports.

REFERENCES

Behnajady M.A., Modirshahla N. and Hamzavi R. (2006) Kinetic study on photocatalytic degradation of C.I. Acid Yellow 23 by ZnO photocatalyst, *J Hazard. Mater. B*, **133**, 226-232.

Behnajady M.A., Modirshahla N., Daneshvar N. and Rabbani M. (2007a) Photocatalytic degradation of an azo dye in a tubular continuous-flow photoreactor with immobilized TiO_2 on glass plates, *Chem. Eng. J*, **127**, 167-176.

Behnajady M.A., Modirshahla N., Daneshvar N. and Rabbani M. (2007b) Photocatalytic degradation of C.I. Acid Red 27 by immobilized ZnO on glass plates in continuous-mode, *J Hazard. Mater. B*, **140**, 257-263.

Carp O., Huisman C.L. and Reller A. (2004) Photoinduced reactivity of titanium dioxide, *Prog. Solid State Chem.*, **32**, 33-177.

Coleman H.M., Chiang K. and Amal R. (2005) Effects of Ag and Pt on photocatalytic degradation of endocrine disrupting chemicals in water, *Chem. Eng. J*, **113**, 65-72.

Daneshvar N., Rabbani M., Modirshahla N. and Behnajady M.A. (2004) Kinetic modeling of photocatalytic degradation of Acid Red 27 in UV/TiO_2 process, *J Photochem. Photobiol. A*, **168**, 39-45.

Kondo M.M. and Jardim W.F. (1991) Photodegradation of chloroform and urea using Ag-loaded titanium dioxide as catalyst, *Water Res.*, **25**, 823-827.

Sahoo C., Gupta A.K. and Pal A. (2005) Photocatalytic degradation of Crystal Violet (C.I. Basic Violet 3) on silver ion doped TiO_2, *Dyes Pigments*, **66**, 189-196.

Sakthivel S., Shankar M.V., Palanichamy M., Arabindoo B., Bahnemann D.W. and Murugesan V. (2004) Enhancement of photocatalytic activity by metal deposition: characterisation and photonic efficiency of Pt, Au and Pd deposited on TiO_2 catalyst, *Water Res.*, **38**, 3001-3008.

Sobana N., Muruganadham M. and Swaminathan M. (2006) Nano-Ag particles doped TiO_2 for efficient photodegradation of Direct azo dyes, *J Mol. Catal. A*, **258**, 124-132.

Subba Rao K.V., Lavédrine B. and Boule P. (2003) Influence of metallic species on TiO_2 for the photocatalytic degradation of dyes and dye intermediates, *J Photochem. Photobiol. A*, **154**, 189-193.

Szabó-Bárdos E., Czili H. and Horváth A. (2003) Photocatalytic oxidation of oxalic acid enhanced by silver deposition on a TiO_2 surface, *J Photochem. Photobiol. A*, **154**, 195-201.

Vamathevan V., Amal R., Beydoun D., Low G. and McEvoy S. (2002) Photocatalytic oxidation of organics in water using pure and silver-modified titanium dioxide particles, *J Photochem. Photobiol. A*, **148**, 233-245.

Wu C.-H. (2004) Comparison of azo dye degradation efficiency using UV/single semiconductor and UV/coupled semiconductor systems, *Chemosphere*, **57**, 601-608.